ECONOMICS

Estimating economic damage from climate change in the United States

Solomon Hsiang,[1,2]*† Robert Kopp,[3]*† Amir Jina,[4]† James Rising,[1,5]†
Michael Delgado,[6] Shashank Mohan,[6] D. J. Rasmussen,[7] Robert Muir-Wood,[8]
Paul Wilson,[8] Michael Oppenheimer,[7,9] Kate Larsen,[6] Trevor Houser[6]

Estimates of climate change damage are central to the design of climate policies. Here, we develop a flexible architecture for computing damages that integrates climate science, econometric analyses, and process models. We use this approach to construct spatially explicit, probabilistic, and empirically derived estimates of economic damage in the United States from climate change. The combined value of market and nonmarket damage across analyzed sectors—agriculture, crime, coastal storms, energy, human mortality, and labor—increases quadratically in global mean temperature, costing roughly 1.2% of gross domestic product per +1°C on average. Importantly, risk is distributed unequally across locations, generating a large transfer of value northward and westward that increases economic inequality. By the late 21st century, the poorest third of counties are projected to experience damages between 2 and 20% of county income (90% chance) under business-as-usual emissions (Representative Concentration Pathway 8.5).

Economically rational management of the global climate requires that the costs of reducing greenhouse gas emissions be weighed against the benefits of doing so (or, conversely, the costs of not doing so). A vast literature has considered this problem, developing, among other insights, our understanding of the optimal timing of investments (*1*), the role of uncertainty (*2*), the importance of future adaptation (*3*), the role of trade (*4*), and the potentially large impact of unanticipated tipping points (*5*, *6*). Integrated assessment models that value the benefits of greenhouse gas abatement are used by governments to estimate the social cost of climate change (*7*, *8*), which in turn informs the design of greenhouse gas policies. However, the estimated benefits of greenhouse gas abatement—or conversely, the "damages" from climate change—are conceptually and computationally challenging to construct. Because of this difficulty, previous analyses have relied on rough estimates, theorized effects, or limited process modeling at continental scales or larger (*9*–*11*), with no systematic calibration to observed human-climate linkages (*12*). Since the original development of these models, methodological innovations (*13*) coupled with data availability and computing power have fueled rapid growth in a spatially resolved, empirical understanding of these relationships (*14*). Yet integrated assessments of climate change and their calculation of the social cost of carbon do not reflect these advances (*15*–*17*).

[1]Global Policy Laboratory, Goldman School of Public Policy, University of California, Berkeley, CA, USA. [2]National Bureau of Economic Research, Cambridge, MA, USA. [3]Department of Earth and Planetary Sciences and Institute of Earth, Ocean, and Atmospheric Sciences, Rutgers University, New Brunswick, NJ, USA. [4]Department of Economics and Harris School of Public Policy, University of Chicago, Chicago, IL, USA. [5]Energy Resource Group, University of California, Berkeley, CA, USA. [6]Rhodium Group, New York, NY, USA. [7]Woodrow Wilson School of Public and International Affairs, Princeton University, Princeton, NJ, USA. [8]Risk Management Solutions, Newark, CA, USA. [9]Department of Geosciences, Princeton University, Princeton, NJ, USA.
***Corresponding author. Email: shsiang@berkeley.edu (S.H.); robert.kopp@rutgers.edu (R.K.)** †These authors contributed equally to this work.

Here, we develop an integrated architecture to compute potential economic damages from climate change based on empirical evidence, which we apply to the United States. Our risk-based approach is grounded in empirical longitudinal analyses of nonlinear, sector-specific impacts, supplemented with detailed energy system, inundation, and cyclone models. Built upon a calibrated distribution of downscaled climate models, this approach is probabilistic and highly resolved across geographic space while taking into account the spatial and sectoral covariance of impacts in each possible future. Our framework is designed to continuously integrate new empirical findings and new climate model projections as the supporting subfields of research advance in the future. When applied to the U.S. economy, this approach provides a probabilistic and empirically derived "damage function," linking global mean surface temperature (GMST) to market and nonmarket costs in the United States, built up from empirical analyses using micro-level data.

System architecture

We developed the Spatial Empirical Adaptive Global-to-Local Assessment System (SEAGLAS) to dynamically integrate and synthesize research outputs across multiple fields in near-real time. We use SEAGLAS to construct probabilistic, county-level impact estimates that are benchmarked to GMST changes. [See section A of the supplementary materials (SM) for additional details (*18*).]

County-level projections of daily temperature and precipitation are constructed and sampled following a three-step process that simultaneously captures the probability distribution of climate responses to forcing, spatiotemporal structures within each climate realization, and spatiotemporal autocorrelation of weather (*19*): (i) For each forcing pathway considered [Representative Concentration Pathways (RCPs) 2.6, 4.5, and 8.5] (*20*), a probability distribution for GMST change is constructed based on an estimated distribution of equilibrium climate sensitivity, historical observations, and a simple climate model (SCM) (*19*). (ii) The joint spatiotemporal distribution of monthly temperature and precipitation is constructed from a broad range of global climate models (GCMs), statistically downscaled from the Coupled Model Intercomparison Project 5 (CMIP5) archive (*21*) and assigned a probability of realization such that the distribution of 21st-century GMST change mirrors the distribution from the SCM. Tails of the distribution beyond the range present in the CMIP5 archive are represented by "model surrogates" constructed by scaling patterns from CMIP5 models using the GMST projections from the SCM. Together, we refer to the union of monthly resolution GCM and model surrogate output as the set of climate realizations that are each weighted to reflect a single probability distribution (Fig. 1A). These weights are used when we compute damage probability distributions for specific RCP scenarios. (iii) We then construct a set of 10 daily projections for each climate realization by superimposing daily weather residuals relative to monthly climatologies that are resampled in yearly blocks from the period 1981 to 2010 (Fig. 1B).

A distribution of empirically grounded economic impacts is computed for each joint realization of county-level daily temperature and precipitation: (iv) Econometrically derived dose-response functions (*13*) estimating the nonlinear effects of temperature, rainfall, and CO_2 on agriculture (*22*, *23*), mortality (*24*, *25*), crime (*26*, *27*), labor (*28*), and energy demand (*24*) are constructed via Bayesian meta-analysis (*29*) (e.g., Fig. 1, C to H, and SM sections B and C). Following the approach and criteria laid out in (*30*), we only employ studies that are nationally representative, spatially disaggregated, and account for temporal displacement and unobserved heterogeneity across locations, along with the additional criterion that studies statistically identify marginal distortions in the distribution of experienced daily temperatures (*13*, *14*). (v) Econometric uncertainty is accounted for by resampling from the 26 posterior functions in (iv) (fig. S4). (vi) County-level daily projections from (iii) are mapped onto the distribution of possible responses from (v) to construct 3143 county-level joint distributions for 15 impacts across 29,000 possible states of the world during 2000 to 2099 (SM sections D and E), although for display purposes we primarily summarize 2080 to 2099 impacts here.

A parallel approach is necessary to estimate energy demand changes and coastal impacts: (vii) Energy demand estimated in (iv) is used as a partial calibration for the National Energy Modeling System (NEMS) (*31*) (SM section G). NEMS is then run with different weather realizations to estimate energy supply costs. (viii) Cyclone exposure is simulated via analytical wind field models (*32*) that force a storm surge model (*33*), with cyclogenesis and storm tracks generated via either (i) semiparametrically resampling historical activity (*34*) or (ii) resampling from projected storm tracks and intensities (*35*) (SM section H). (ix) Inundation from localized probabilistic sea level rise projections (*36*) interacting with storm surge and wind exposure in (viii) are mapped onto a database of all coastal properties maintained by Risk Management Solutions, where engineering models predict damage (SM section H).

Finally, economic impacts are aggregated and indexed against the GMST in their corresponding climate realization to construct multidimensional probabilistic damage functions suitable for application in integrated assessment modeling: (x) Direct impacts from (vi), (vii), and (ix) are aggregated across space or time within each sector. Monetizing the value of nonmarket impacts (deaths and crime) using willingness-to-pay or accounting estimates (*37*, *38*), impacts across all sectors are aggregated to compute total damages (SM sections I and J).

Importantly, for clarity, our approach holds the scale and spatial distribution of the U.S. population and economy fixed at values observed in 2012, since current values are well understood and widely agreed on. Various previous analyses [e.g., (*39*)] note that natural demographic change and economic growth may dominate climate change effects in overall magnitude, although such comparisons are not our focus here. Because we compute impacts using scale-free intensive measures (e.g., percentage changes), future expansion of the economy or population does not affect our county-level estimates, and our aggregate results will be unbiased as long as this expansion is balanced across space. If such expansion is not balanced across space, then our aggregated results will require a second-order adjustment with a sign that depends on the spatial covariance of changes in climate exposure and changes in economic or population structure, as shown in (*40*). In previous work (*41*), we demonstrated how results for some direct impacts might change if future rates of adaptation to climate mirror historical patterns and rates. The paucity of existing quantitative studies on adaptation prevents us from currently applying this approach to all sectors, although such additions are expected in future work.

Distribution of costs and benefits

Standard approaches to valuing climate damage describe average impacts for large regions (e.g., North America) or the entire globe as a whole. Yet examining county-level impacts reveals major redistributive impacts of climate change on some sectors that are not captured by regional or global averages. Figure 2 and fig. S2 display the median average impact during the period 2080 to 2099 due to climate changes in RCP8.5, a trajectory consistent with fossil-fuel–intensive economic growth, for each county. In cases where responses to temperature are nonlinear (e.g., Fig. 1, C, E, and H), the current climate of counties affects

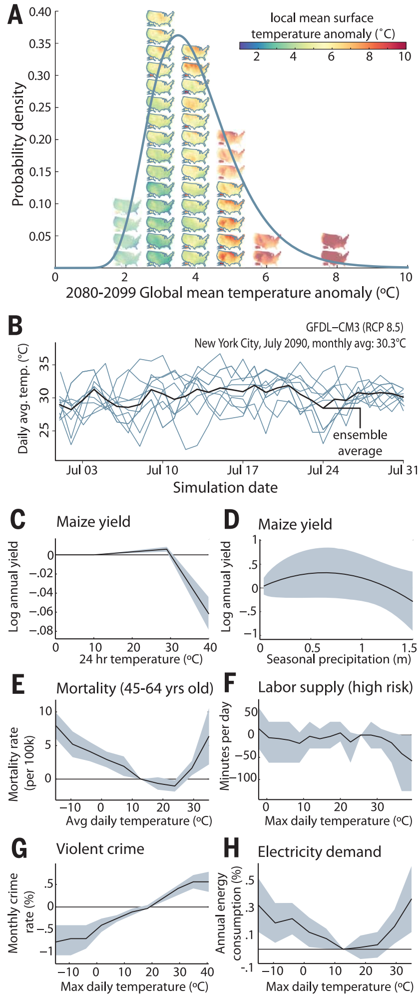

Fig. 1. Recombining previous research results as composite inputs to SEAGLAS. (**A**) Forty-four climate models (outlined maps) and model surrogates (dimmed maps) are weighted so that the distribution of the 2080 to 2099 GMST anomaly exhibited by weighted models matches the probability distribution of estimated GMST responses (blue-gray line) under RCP8.5. Analogous display for precipitation in fig. S1. (**B**) Example of 10 months of daily residuals in New York City, block resampled from historical observations at the same location and superimposed on monthly mean projections for a single model (GFDL-CM3) and scenario (RCP8.5) drawn from (A). (**C** to **H**) Examples of composite (posterior) county- level dose-response functions derived from nonlinear Bayesian meta-analysis of empirical studies based on selection criteria in (*30*). Median estimate is black, central 95% credible interval is blue-gray. To construct probabilistic impact projections, responses for each category are independently resampled from each distribution of possible response functions and combined with resampled climate realizations, as in (A), and weather realizations, as in (B). [(C) and (D)] Estimated causal effect of (C) 24 hours temperature and (D) seasonal rainfall on maize yields. (E) Daily average temperature on all-cause mortality for the 45- to 64-year-old population. (F) Daily maximum temperature on daily labor supply in high-risk industries exposed to outdoor temperatures. [(G) and (H)] Daily maximum temperature on (G) monthly violent crime rates and (H) annual residential electricity demand. All sources are detailed in SM section B.

whether additional warming generates benefits, has limited effect, or imposes costs. For example, warming reduces mortality in cold northern counties and elevates it in hot southern counties (Fig. 2B). Sectors with roughly linear responses, such as violent crime (Fig. 1G), have more uniform effects across locations (Fig. 2H). Atlantic coast counties suffer the largest losses from cyclone intensification and mean sea level (MSL) rise (Fig. 2F and fig. S10). In general (except for crime and some coastal damages), Southern and Midwestern populations suffer the largest losses, while Northern and Western populations have smaller or even negative damages, the latter amounting to net gains from projected climate changes.

Combining impacts across sectors reveals that warming causes a net transfer of value from Southern, Central, and Mid-Atlantic regions toward the Pacific Northwest, the Great Lakes region, and New England (Fig. 2I). In some counties, median losses exceed 20% of gross county product (GCP), while median gains sometimes exceed 10% of GCP. Because losses are largest in regions that are already poorer on average, climate change tends to increase preexisting inequality in the United States. Nationally averaged effects, used in previous assessments, do not capture this subnational restructuring of the U.S. economy.

Nationally aggregated sectoral impacts

We recover sector-specific damages as a function of GMST change by nationally aggregating county-level impacts within each state of the world defined by an RCP scenario, climate realization, resampled weather, and econometrically derived parameter estimate (SM sections D and E). The distribution of sectoral impacts is compared with GMST change in each realization in Fig. 3 (SM section J). Although several sectors exhibit micro-level responses that are highly nonlinear with respect to county temperature (e.g., Fig. 1C), aggregated damages exhibit less-extreme curvature with respect to GMST change, as was hypothesized and derived in (*42*).

Average yields in agriculture decline with rising GMST, but higher CO_2 concentrations offset much of the loss for the coolest climate realizations in each of the three RCP scenarios. Accounting for estimated effects of CO_2 fertilization (SM section B) and precipitation, warming still dominates, reducing national yields ~9.1 (±0.6 SEM) % per °C (Fig. 3A). Because effects of CO_2 are highly uncertain and not derived using the same criteria as other effects, we evaluate the sensitivity of these projections by computing losses without CO_2 fertilization (Fig. 3B) and find that temperature and rainfall changes alone would be expected

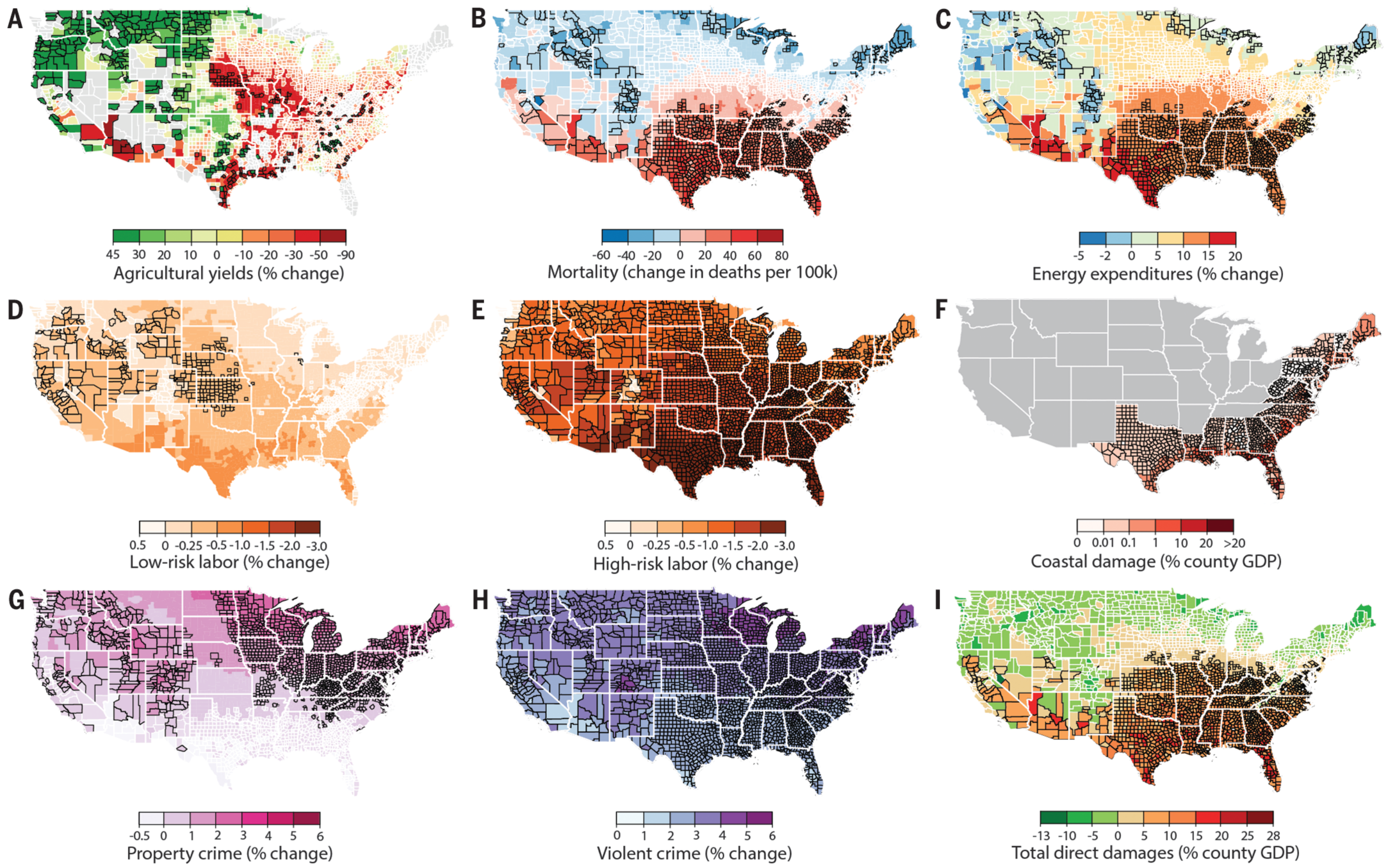

Fig. 2. Spatial distributions of projected damages. County-level median values for average 2080 to 2099 RCP8.5 impacts. Impacts are changes relative to counterfactual "no additional climate change" trajectories. Color indicates magnitude of impact in median projection; outline color indicates level of agreement across projections (thin white outline, inner 66% of projections disagree in sign; no outline, ≥83% of projections agree in sign; black outline, ≥95% agree in sign; thick white outline, state borders; maps without outlines shown in fig. S2). Negative damages indicate economic gains. (**A**) Percent change in yields, area-weighted average for maize, wheat, soybeans, and cotton. (**B**) Change in all-cause mortality rates, across all age groups. (**C**) Change in electricity demand. (**D**) Change in labor supply of full-time-equivalent workers for low-risk jobs where workers are minimally exposed to outdoor temperature. (**E**) Same as (D), except for high-risk jobs where workers are heavily exposed to outdoor temperatures. (**F**) Change in damages from coastal storms. (**G**) Change in property-crime rates. (**H**) Change in violent-crime rates. (**I**) Median total direct economic damage across all sectors [(A) to (H)].

to reduce yields ~12.1 (±0.7) % per °C (see also figs. S11 and S12 and tables S10 and S11).

Rising mortality in hot locations more than offsets reductions in cool regions, so annual national mortality rates rise ~5.4 (±0.5) deaths per 100,000 per °C (Fig. 3C). For lower GMST changes, this is driven by mortality between ages 1 and 44 and by infant mortality and ages ≥45 for larger GMST increases (fig. S13 and table S12).

Electricity demand rises on net for all GMST changes, roughly 5.3 (± 0.14) % per °C, because rising demand from hot days more than offsets falling demand on cool days (Fig. 3D and table S13). Because total costs in the energy sector are computed using NEMS, demand is not statistically resampled as other sectors are (SM section G).

Total hours of labor supplied declines ~0.11 (±0.004) % per °C in GMST for low-risk workers, who are predominantly not exposed to outdoor temperatures, and 0.53 (±0.01) % per °C for high-risk workers who are exposed (~23% of all employed workers, in sectors such as construction, mining, agriculture, and manufacturing) (Fig. 3, E and F, and table S14).

Property crime increases as the number of cold days—which suppress property crime rates (fig. S4)—falls but then flattens for higher levels of warming because hot days do not affect property crime rates. Violent crime rates increase linearly at a relatively precise 0.88 (±0.04) % per °C in GMST (Fig. 3, G and H, and table S15).

Coastal impacts are driven by the amplification of tropical cyclone and extratropical cyclone storm tides by local MSL rise and by the alteration of the frequency, distribution, and intensity of these cyclones (SM section H). Rising MSL increases the storm tide height and floodplain during cyclones: Fig. 4, A to D, illustrates how 1-in-100-year floodplains evolve over time due to MSL rise (RCP8.5) with and without projected changes in cyclones for two major coastal cities. Coastal impacts are distributed highly unequally, with acute impacts for eastern coastal states with topographically low cities; MSL rise alone raises expected direct annual economic damage 0.6 to 1.3% of state gross domestic product (GDP) for South Carolina, Louisiana, and Florida in the median case, and 0.7 to 2.3% for the 95th percentile of MSL rise (Fig. 4E) (RCP8.5). Nationally, MSL rise would increase annual expected storm damages roughly 0.0014% GDP per cm if capital and storm frequency remain fixed (Fig. 4F). Accounting for the projected alteration of the TC distribution roughly doubles the damage from MSL rise, the two combined costing an estimated additional 0.5 (±0.2) % of GDP annually in 2100 when aggregated nationally (Fig. 4G).

Uncertainty

At the county level, conditional upon RCP, uncertainty in direct damages is driven by climate uncertainty (both in GMST and in the expected spatiotemporal distribution of changes conditional on GMST), by within-month weather exposure, and by statistical assumptions and sampling used to derive dose-response functions, as well as by

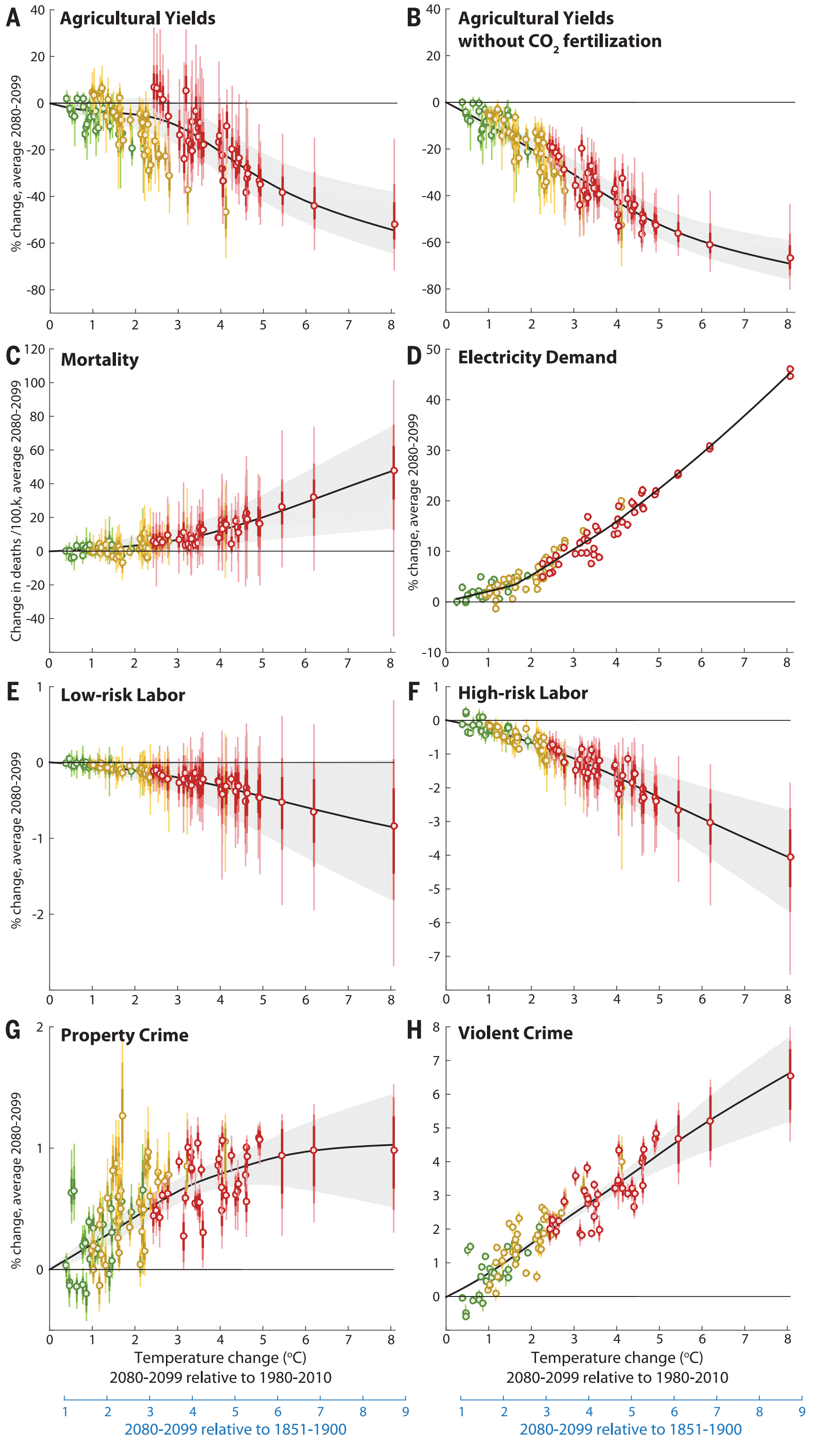

Fig. 3. Probabilistic national aggregate damage functions by sector. Dot-whiskers indicate the distribution of direct damages in 2080 to 2099 (averaged) for multiple realizations of each combination of climate models and scenario projection (dot, median; dark line, inner 66% credible interval; medium line, inner 90%; light line, inner 95%). Green are from RCP2.6, yellow from RCP4.5, red from RCP8.5. Distributions are located on the horizontal axis according to GMST change realized in each model-scenario combination (blue axis is change relative to preindustrial). Black lines are restricted cubic spline regressions through median values, and gray shaded regions are bounded (above and below) by restricted cubic spline regressions through the 5th and 95th quantiles of each distribution, all of which are restricted to intercept the origin. (**A**) Total agricultural impact accounting for temperature, rainfall, and CO_2 fertilization (CO_2 concentration is uniform within each RCP, causing discontinuities across scenarios). (**B**) Without CO_2 effect. (**C**) All-cause mortality for all ages. (**D**) Electricity demand used in process model, which does not resample statistical uncertainty (SM section G). (**E** and **F**) Labor supply for (E) low-risk and (F) high-risk worker groups. (**G**) Property-crime rates. (**H**) Violent-crime rates.

uncertainty generated by the interaction of these factors. Figure 2 displays county-level uncertainty in the impact on each sector by indicating the level of agreement among 11,000 projections on the overall sign of impacts in each county. Notably, process models (e.g., NEMS) and other variables, such as baseline work hours or the VSL, contain uncertainty that remains uncharacterized.

Aggregating results nationally, we decompose uncertainty into contributions from climate, within-month weather, and dose-response relationships by resampling each individually while holding the others fixed (*43*), recovering how these variances combine to produce the total variance across projections (figs. S6 and S7). In general, climate uncertainty dominates, contributing 41 to 104% of the total variance by end of century, with econometric uncertainty in low-risk labor (88% of total variance) being the only exception. Within-month weather uncertainty has a negligible effect on 20-year averages. The interaction between climate and dose-response uncertainty also contributes to the total variance (negatively in some cases), because impact functions are nonlinear (SM section F).

Nationally aggregated total damage

Impacts across sectors can be aggregated into a single measure of overall economic damage if suitable values can be assigned to each impact category. For nonmarket costs, we use current U.S. Environmental Protection Agency values for the value of a statistical life (*37*) and published estimates for the cost of crime (*38*), which we combine with current average market valuations of market impacts (SM section I). Summing across impacts, we estimate the conditional distribution of total direct damages as a function of GMST change (Fig. 5A), finding that expected annual losses increase by ~0.6% GDP per 1°C at +1°C of GMST warming (relative to 1981 to 2010) to 1.7% GDP per 1°C at +5°C GMST (SM section J). This response is well approximated by a quadratic function (fig. S14) that is highly statistically significant for changes above 1°C ($P < 0.001$) (table S16). Combined uncertainty in aggregate impacts grows with warming, so the very likely (5th to 95th percentile) range of losses at 1.5°C of warming is –0.1 to 1.7% GDP, at 4°C of warming is 1.5 to 5.6% GDP, and at 8°C warming is 6.4 to 15.7% GDP annually (gray band, Fig. 5A and table S17). Approximating this damage function with a linear

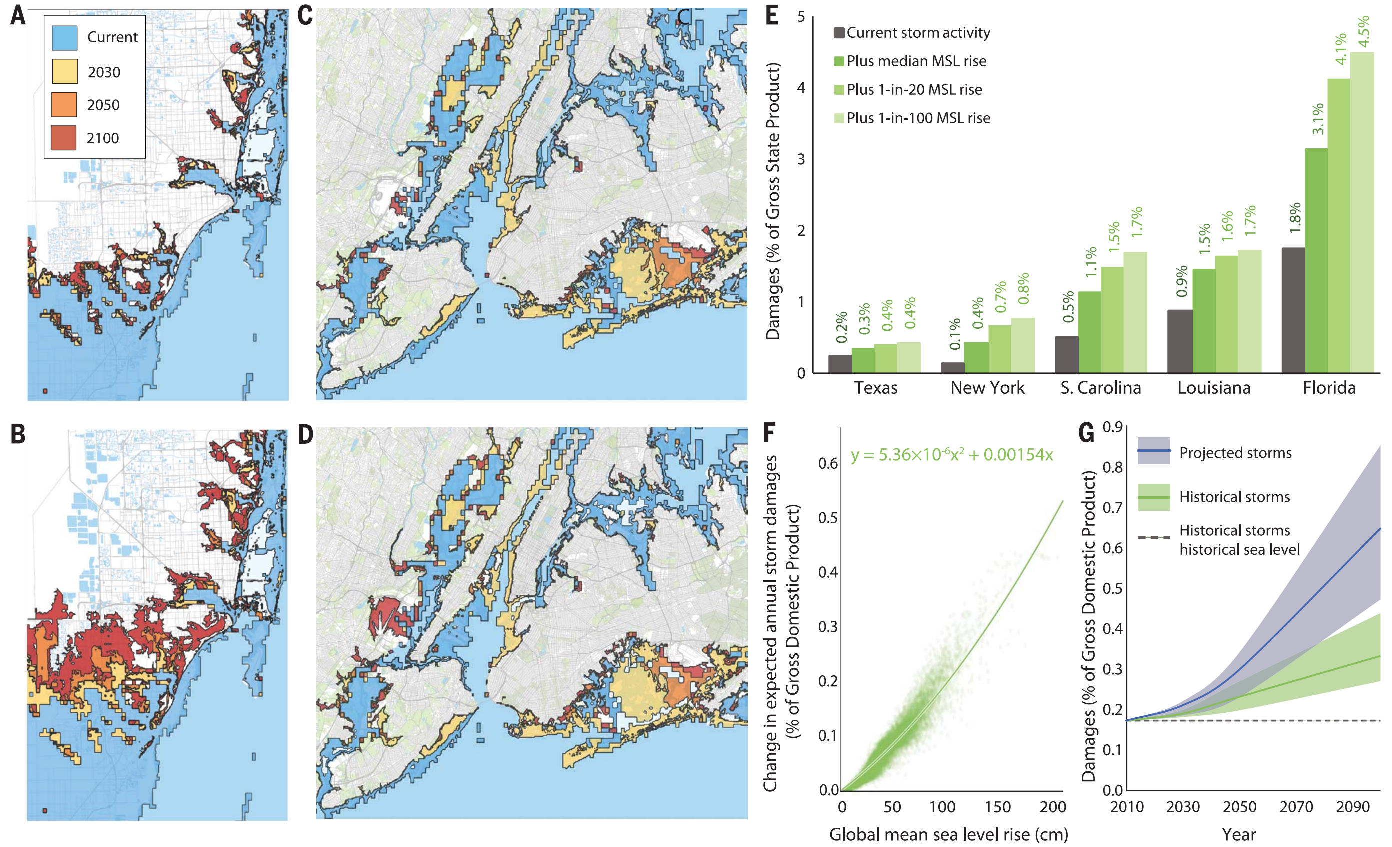

Fig. 4. Economic costs of sea level rise interacting with cyclones. (**A**) Example 100-year floodplain in Miami, Florida, under median sea level rise for RCP8.5, assuming no change in tropical cyclone activity. (**B**) Same, but accounting for projected changes in tropical cyclone activity. (**C**) Same as (A), but for New York, New York. (**D**) Same as (B), but for New York, New York. (**E**) Annual average direct property damages from tropical cyclones and extratropical cyclones in the five most-affected states, assuming that installed infrastructure and cyclone activity is held fixed at current levels. Bars indicate capital losses under current sea level, median, 95th-percentile and 99th-percentile sea level rise in RCP8.5 in 2100. (**F**) Nationally aggregated additional annual damages above historical versus global mean sea level rise holding storm frequency fixed. (**G**) Annual average direct property damages nationally aggregated in RCP8.5, incorporating mean sea level rise and either historical or projected tropical cyclone activity. Historical storm damage is the dashed line.

form suggests losses of ~1.2% GDP per 1°C on average in our sample of scenarios (table S16).

The greatest direct cost for GMST changes larger than 2.5°C is the burden of excess mortality, with sizable but smaller contributions from changes in labor supply, energy demand, and agricultural production (Fig. 5B). Coastal storm impacts are also sizable but do not scale strongly with GMST because projections of global MSL are dependent on RCP but are not explicitly calculated as functions of GMST (*36*), causing the coastal storm contribution to the slope of the damage function to be relatively muted. It is possible to use alternative approaches to valuing mortality in which the loss of lives for older and/or low-income individuals are assigned lower value than those of younger and/or high-income individuals (*44*), an adjustment that would alter damages differently for different levels of warming based on the age and income profile of affected individuals (e.g., fig. S13). Here, we focus on the approach legally adopted by the U.S. government for environmental cost-benefit analysis, in which the lives of all individuals are valued equally (*37*). Because the VSL parameter is influential, challenging to measure empirically, and may evolve in the future, its influence on damages is an important area for future investigation.

Risk and inequality of total local damages

Climate change increases the unpredictability and between-county inequality of future economic outcomes, effects that may alter the valuation of climate damages beyond their nationally averaged expected costs (*45*). Figure 5C displays the probability distribution of damage under RCP8.5 as a fraction of county income, ordering counties by their current income per capita. Median damages are systematically larger in low-income counties, increasing by 0.93% of county income (95% confidence interval = 0.85 to 1.01%) on average for each reduction in current income decile. In the richest third of counties, the average very likely range (90% credible interval, determined as the average of 5th and 95th percentile values across counties) for damages is –1.2 to 6.8% of county income (negative damages are benefits), whereas for the poorest third of counties, the average range is 2.0 to 19.6% of county income. These differences are more extreme for the richest 5% and poorest 5% of counties, with average intervals for damage of –1.1 to 4.2% and 5.5 to 27.8%, respectively.

We note that it is possible to adjust the aggregate damage function in Fig. 5A to capture societal aversion to both the risk and inequality in Fig. 5C. In SM section K, we demonstrate one approach to constructing such inequality-neutral, certainty-equivalent damage functions. Depending on the parameters used to value risk and inequality, accounting for these factors may dramatically influence society's valuation of damages in a manner similar to the large influence of discount rates on the valuation of future damages (*46*). This finding highlights risk and inequality valuation as critical areas for future research.

Discussion

Our results provide a probabilistic, national damage function based on spatially disaggregated, empirical, longitudinal analyses of climate impacts and available global climate models, but it will not be the last estimate. Because we use stringent selection criteria for empirical studies,

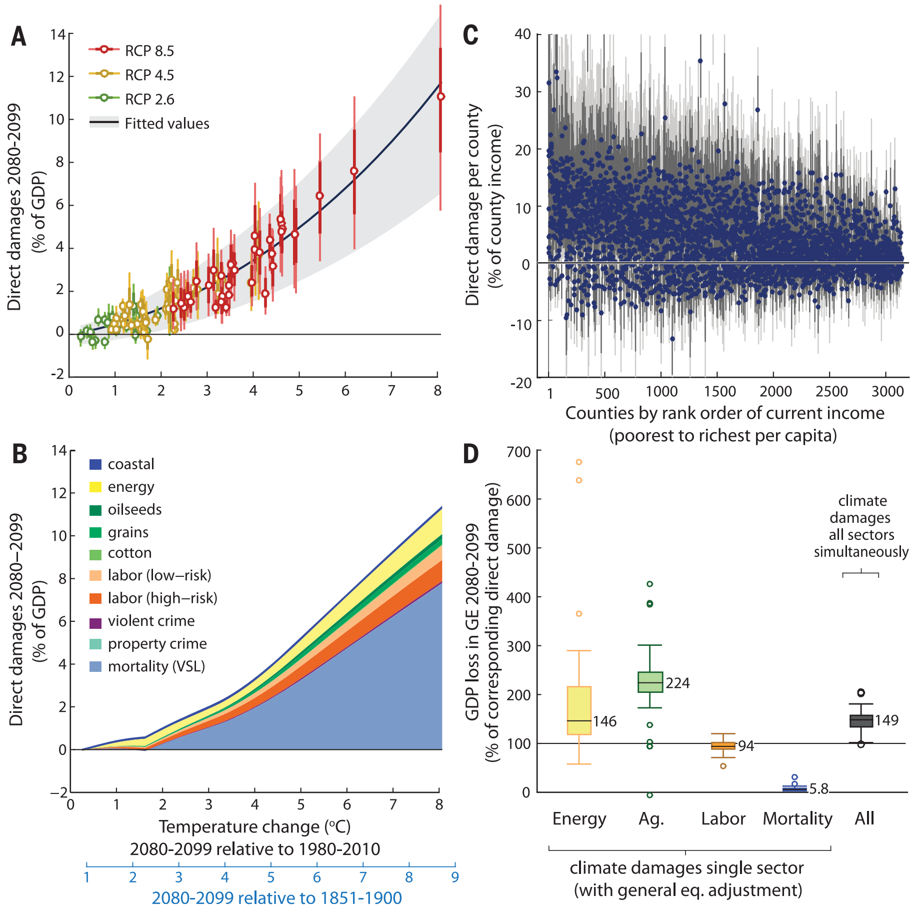

Fig. 5. Estimates of total direct economic damage from climate change. (**A**) Total direct damage to U.S. economy, summed across all assessed sectors, as a function of global mean temperature change. Dot-whisker markers as in Fig. 3. The black line is quadratic regression through all simulations (damage = 0.283 ΔGMST + 0.146 ΔGMST^2); the shaded region is bounded by quantile regressions through the 5th and 95th percentiles. Alternative polynomial forms and statistical uncertainty are reported in fig. S14 and tables S16 and S17. (**B**) Contributions to median estimate of aggregate damage by impact category. (Coastal impacts do not scale with temperature.) (**C**) Probability distribution damage in each of 3143 U.S. counties as a fraction of county income, ordered by current county income. Dots, median; dark whiskers, inner 66% credible interval; light whiskers, inner 90%. (**D**) Distributions of GDP loss compared with direct damages when a CGE model is forced by direct damages each period. Black line, median (labeled); boxes, interquartile range; dots, outliers. Energy, Ag., Labor, and Mortality indicate comparisons when the model is forced by damages only in the specified sector and GDP losses are compared with direct damages in that sector under the same forcing. CGE mortality only affects GDP through lost earnings, but direct mortality damages in (A) to (C) account for nonmarket VSL. "All" indicates the ratio of total costs (excluding mortality for consistency) in complete simulations where all sectors in the CGE model are forced by direct damages simultaneously.

there are multiple known sectors of the U.S. economy for which no suitable studies exist and were thus omitted from this analysis [e.g., effects of morbidity (*47*), worker productivity (*48*), or biodiversity loss (*49*)]. The SEAGLAS architecture is constructed around the idea that rigorous future studies will quantify climate impacts in these "missing sectors" and thus should be included in future assessments. Our approach therefore allows for updating based on new econometric results or climate model projections, and our results should be interpreted as current best estimates that will be dynamically adjusted as research in the community advances.

We stress that the results presented here are projections relative to a counterfactual baseline economic trajectory that is unknown and will evolve based on numerous factors unrelated to climate change. As constructed, knowledge of this baseline trajectory is not essential to estimating the relative first-order impact imposed by climate change.

We should expect that populations will adapt to climate change in numerous ways (*14*). Some actions, such as use of air conditioning (*25*), likely limit the impact of climatic exposure, whereas other actions, such as social conflict (*30*), likely exacerbate impacts. Because the empirical results that we use describe how populations have actually responded to climatic conditions in the past, our damage estimates capture numerous forms of adaptation to the extent that populations have previously employed them (*50*). For example, if farmers have been adjusting their planting conditions based on observable rainfall, the effect of these adjustments will be captured by our results. Although, if there are trends in adaptive behaviors, previously unobserved adaptation "tipping points," or qualitative gains in adaptation-related technologies, then our findings may require adjustment. In previous work, we demonstrated how to employ empirical approaches to project trends in adaptive behaviors and recomputed impacts in some sectors (*41*), but sufficient data do not yet exist to estimate these effects in all the sectors we cover here. Yet in cases where sufficient data do exist to simulate these adaptations, the net effect of this correction is small in magnitude relative to the large uncertainty that is introduced by such adjustments (*41*), a result of the high uncertainty in current estimates for trends in adaptation (*25*, *51*).

As mentioned above, populations may move across space in response to altered climate conditions. This response will not alter our local projections, but it will cause our estimates to over- or underpredict nationally aggregated impacts, depending on the spatial covariance between population changes and local economic losses caused by climate change. This adjustment will tend to be second order relative to the direct effect of climate change (*13*); nonetheless, accounting for this adjustment is an area for future investigation.

Another possible adjustment that may occur in response to climate damages is for the economy to reallocate nonlabor resources, partially shifting the locations of economic activity, to cope with these changes. We consider the extent to which this response might alter the direct economic damages that we characterize above by developing a computable general equilibrium (CGE) model that reallocates capital across locations and industries in response to the capital and productivity losses described above during each period of a century-long integration (SM section L). Theoretically, it is possible for these reallocations to reduce damages, as production migrates away from adverse climates, or for them to increase damages, as losses in one location alter economic decisions in other locations and/or later periods by influencing markets through prices. We simulate the trajectory of the future economy under each RCP8.5 climate realization, imposing our computed direct damages each period. When direct damages are imposed on only one sector at a time, the total end-of-century economic loss may be larger or smaller than the corresponding direct damages estimate, depending on the sector and climate realization (Fig. 5D). Market costs of mortality computed with this approach are dramatically lower than nonmarket costs described above because the foregone earnings in the market equilibrium are much smaller than the VSL used to compute direct damages. Overall, in a complete simulation where national markets are simultaneously forced by direct damages in all sectors, net market losses in general equilibrium tend to be larger than direct damages by ~50% (mortality is excluded from both). These simulations are relatively coarse approximations of the complex national economy and do not capture international trade effects, but they suggest that the spatial reallocation of economic activity within the United States may not easily mitigate the economic damage from climate change.

Our results are "bottom-up" micro-founded estimates of U.S. damages, although parallel analyses have employed "top-down" macro-level approaches that estimate how overall productivity measures (such as GDP) directly respond to temperature or cyclone changes without knowledge of the underlying mechanisms generating those losses. This alternative approach can be compared to our estimates of market losses only, as they will not account for nonmarket valuations. Our market estimates are for a 1.0 to 3.0% loss of annual national average GDP under RCP8.5 at the end of the century. Previous top-down county-level analysis of productivity estimates that national output would decline 1.2 to 3.1% after 20 years of exposure to RCP8.5 temperatures at the end of the century (*52*). In top-down global analyses of all countries, the 10.3% intensification of average U.S. tropical cyclone exposure in emissions scenario A1B (roughly comparable to RCP8.5) (*35*) is estimated to reduce GDP ~0.09% per year (*53*) (not accounting for MSL rise), and the cumulative effect of linear national warming by an additional 1°C over 75 years is estimated to reduce GDP ~2.9% (2080 to 2099 average) (*42*). In comparison, we estimate that losses to cyclone intensification are ~0.07% of annual GDP per 1°C in global mean temperature change and that economy-wide direct damages are ~1.2% of annual GDP per year per 1°C. Overall, such comparisons suggest that top-down and bottom-up empirical estimates are beginning to converge, although important differences—in accounting procedures as well as recovered magnitudes and temporal structure—remain. Future investigation should reconcile these differences.

We have focused on the U.S. economy, although the bulk of the economic damage from climate change will be borne outside of the United States (*42*), and impacts outside the United States will have indirect effects on the United States through trade, migration, and possibly other channels. In ongoing work, we are expanding SEAGLAS to cover the global economy and to account for additional sectors, such as social conflict (*30*), in order to construct a global damage function that is essential to estimating the global social cost of carbon and designing rational global climate policies (*7*, *9*).

REFERENCES AND NOTES

1. W. D. Nordhaus, *Am. Econ. Rev.* **83**, 313–317 (1993).
2. M. L. Weitzman, *Rev. Econ. Stat.* **91**, 1–19 (2009).
3. K. C. de Bruin, R. B. Dellink, R. S. Tol, *Clim. Change* **95**, 63–81 (2009).
4. A. Costinot, D. Donaldson, C. Smith, *J. Polit. Econ.* **124**, 205–248 (2016).
5. D. Lemoine, C. Traeger, *Am. Econ. J. Econ. Policy* **6**, 137–166 (2014).
6. Y. Cai, K. L. Judd, T. M. Lenton, T. S. Lontzek, D. Narita, *Proc. Natl. Acad. Sci. U.S.A.* **112**, 4606–4611 (2015).
7. N. Stern, *Stern Review: The Economics of Climate Change* (Cambridge Univ. Press, 2006).
8. Interagency Working Group on Social Cost of Carbon, Technical support document: Social cost of carbon for regulatory impact analysis under Executive Order 12866, *Tech. rep.*, United States Government (2010).
9. R. L. Revesz *et al.*, *Nature* **508**, 173–175 (2014).
10. N. Stern, *J. Econ. Lit.* **51**, 838–859 (2013).
11. R. S. Tol, *J. Econ. Perspect.* **23**, 29–51 (2009).
12. R. S. Pindyck, *J. Econ. Lit.* **51**, 860–872 (2013).
13. S. M. Hsiang, *Annu. Rev. Resour. Econ.* **8**, 43–75 (2016).
14. T. A. Carleton, S. M. Hsiang, *Science* **353**, aad9837 (2016).
15. R. E. Kopp, S. M. Hsiang, M. Oppenheimer, *Impacts World 2013 Conference Proceedings* (Potsdam Institute for Climate Impact Research, Potsdam, Germany, 2013), pp. 834–843.
16. W. Pizer *et al.*, *Science* **346**, 1189–1190 (2014).
17. M. Burke *et al.*, *Science* **352**, 292–293 (2016).
18. Materials and methods are available online as supplementary materials.
19. D. Rasmussen, M. Meinshausen, R. E. Kopp, *J. Appl. Meteorol. Climatol.* **55**, 2301–2322 (2016).
20. D. P. van Vuuren *et al.*, *Clim. Change* **109**, 5–31 (2011).
21. K. E. Taylor, R. J. Stouffer, G. A. Meehl, *Bull. Am. Meteorol. Soc.* **93**, 485–498 (2012).
22. W. Schlenker, M. J. Roberts, *Proc. Natl. Acad. Sci. U.S.A.* **106**, 15594–15598 (2009).
23. J. M. McGrath, D. B. Lobell, *Environ. Res. Lett.* **8**, 014054 (2013).
24. O. Deschênes, M. Greenstone, *Am. Econ. J. Appl. Econ.* **3**, 152–185 (2011).
25. A. Barreca, K. Clay, O. Deschênes, M. Greenstone, J. S. Shapiro, *J. Polit. Econ.* **124**, 105–159 (2016).
26. B. Jacob, L. Lefgren, E. Moretti, *J. Hum. Resour.* **42**, 489–527 (2007).
27. M. Ranson, *J. Environ. Econ. Manage.* **67**, 274–302 (2014).
28. J. Graff Zivin, M. Neidell, *J. Labor Econ.* **32**, 1–26 (2014).
29. J. A. Rising, S. M. Hsiang, SSRN Working Paper 2458129; available at SSRN: https://ssrn.com/abstract=2458129 (2014).
30. S. M. Hsiang, M. Burke, E. Miguel, *Science* **341**, 1235367 (2013).
31. U.S. Energy Information Administration, The national energy modeling system: An overview, Tech. Rep. DOE/EIA-0581 (2009); www.eia.gov/outlooks/aeo/nems/overview/index.html.
32. H. Willoughby, R. Darling, M. Rahn, *Mon. Weather Rev.* **134**, 1102–1120 (2006).
33. I. Warren, H. Bach, *Environ. Softw.* **7**, 229–240 (1992).
34. T. M. Hall, S. Jewson, *Tellus, Ser. A, Dyn. Meterol. Oceanogr.* **59**, 486–498 (2007).
35. K. A. Emanuel, *Proc. Natl. Acad. Sci. U.S.A.* **110**, 12219–12224 (2013).
36. R. E. Kopp *et al.*, *Earths Futur.* **2**, 383–406 (2014).
37. U.S. Environmental Protection Agency, National Center for Environmental Economics, Valuing mortality risk reductions for environmental policy: A white paper, *Tech. rep.* (2010).
38. P. Heaton, *Hidden in Plain Sight* (RAND Corporation, 2010).
39. C. J. Vörösmarty, P. Green, J. Salisbury, R. B. Lammers, *Science* **289**, 284–288 (2000).
40. S. M. Hsiang, Essays on the social impacts of climate, Ph.D. thesis, Columbia University (2011).
41. T. Houser *et al.*, *Economic Risks of Climate Change: An American Prospectus* (Columbia Univ. Press, 2015).
42. M. Burke, S. M. Hsiang, E. Miguel, *Nature* **527**, 235–239 (2015).
43. E. Hawkins, R. Sutton, *Bull. Am. Meteorol. Soc.* **90**, 1095–1107 (2009).
44. W. K. Viscusi, J. E. Aldy, *J. Risk Uncertain.* **27**, 5–76 (2003).
45. C. Gollier, *Pricing the Planet's Future: The Economics of Discounting in an Uncertain World* (Princeton Univ. Press, 2013).
46. M. L. Weitzman, *J. Econ. Lit.* **45**, 703–724 (2007).
47. J. A. Patz, D. Campbell-Lendrum, T. Holloway, J. A. Foley, *Nature* **438**, 310–317 (2005).
48. S. M. Hsiang, *Proc. Natl. Acad. Sci. U.S.A.* **107**, 15367–15372 (2010).
49. G.-R. Walther *et al.*, *Nature* **416**, 389–395 (2002).
50. O. Deschênes, M. Greenstone, *Am. Econ. Rev.* **97**, 354–385 (2007).
51. M. Burke, K. Emerick, *Am. Econ. J. Econ. Policy* **8**, 106–140 (2016).
52. T. Deryugina, S. M. Hsiang, NBER Working Paper 20750 (NBER, 2014); www.nber.org/papers/w20750.
53. S. M. Hsiang, A. Jina, NBER Working Paper 20352 (NBER, 2014); www.nber.org/papers/w20352.

ACKNOWLEDGMENTS

This research was funded by grants from the National Science Foundation, the U.S. Department of Energy, Skoll Global Threats Fund, and by a nonpartisan grant awarded jointly by Bloomberg Philanthropies, the Office of Hank Paulson, and Next Generation. The methodology and results presented represent the views of the authors and are fully independent of the granting organizations. We thank M. Auffhammer, M. Meinshausen, K. Emanuel, J. Graff Zivin, O. Deschênes, J. McGrath, L. Lefgren, M. Neidell, M. Ranson, M. Roberts, A. Norris, K. Chadha, A. Dobbin, A. Guerrero, L. Schick, and W. Schlenker for providing data and additional analysis; M. Burke, W. Fisk, N. Stern, W. Nordhaus, T. Broccoli, M. Huber, T. Rutherford, J. Buzan, K. Fisher-Vanden, M. Light, D. Lobell, M. Greenstone, K. Hayhoe, G. Heal, D. Holtz-Eakin, J. Samet, A. Schreiber, W. Schlenker, J. Shapiro, M. Spence, L. Linden, L. Mearns, S. Ringstead, G. Yohe, and seminar participants at Duke, MIT, Stanford, the University of Chicago, and the National Bureau of Economic Research (NBER) for important discussions and advice; and J. Delgado and S. Shevtchenko for invaluable technical assistance. Rhodium Group is a private economic research company that conducts independent research for clients in the public, private, and philanthropic sectors. Risk Management Solutions is a catastrophe risk modeling company that provides hazard modeling services to financial institutions and public agencies. The analysis contained in this research article was conducted independently of any commercial work and was not influenced by clients of either organization. Data and code used in this analysis can be obtained at https://zenodo.org/communities/economic-damage-from-climate-change-usa/. S.H. and R.K. conceived of the study. All authors designed the analysis. R.K. and D.J.R. developed climate projections. A.J. and S.H. gathered and reanalyzed econometric results. J.R. developed the meta-analysis system. S.H., R.K., A.J., J.R., M.D., and T.H. designed the economic projection systems, and J.R. developed it with support from M.D. and A.J. T.H., M.D., and S.M. developed the energy modeling system, with econometric support from A.J. R.M.-W., P.W., S.H., R.K., and T.H. designed the approach for analyzing cyclone losses; P.W. and R.M.-W. conducted modeling; and M.D. and A.J. analyzed results. M.D., S.M., and T.H. implemented general equilibrium modeling; R.K., S.H., A.J., and J.R. contributed to its design; and M.D., A.J., and S.H. analyzed the output. J.R. developed and implemented the approach for analyzing uncertainty. A.J. conducted analysis and construction of aggregate damage functions. R.K., S.H., and A.J. developed and implemented the approach for valuing risk and inequality of damages. S.H., R.K., A.J., J.R., M.D., D.J.R., K.L., and T.H. designed the figures; D.J.R. and A.J. constructed Fig. 1; M.D. and T.H. constructed Fig. 4; and A.J. constructed Figs. 2, 3, and 5. All authors wrote the manuscript.

SUPPLEMENTARY MATERIALS

www.sciencemag.org/content/356/6345/1362/suppl/DC1
Materials and Methods
Figs. S1 to S18
Tables S1 to S19
References (*54*–*91*)

21 November 2016; accepted 2 June 2017
10.1126/science.aal4369